International Research Journal of Engineering and Technology (IRJET) e-ISSN: 2395-0056
Volume: 09 Issue: 02 | Feb 2022 www.irjet.net p-ISSN: 2395-0072

Thermal Stability Investigation and Improvement: A Gateway to High Efficiency Organometal Trihalide Perovskite Solar Cells

Chisom Patrick Mbachu[1,2], James Ondoma Onojo[2], Samuel Okechukwu Okozi[2], Matthew Olubiwe[2], Isdore Onyema Akwukwaaegbu and Nsan-Awaji Peterson Ene-Nte[2]

[1]African Center of Excellence in Future Energies and Electrochemical Systems (ACE-FUELS), Federal University of Technology, Owerri, Nigeria.
[2]Department of Electrical /Electronic Engineering, Federal University of Technology, Owerri, Nigeria

---

Abstract - *Organometal Trihalide Perovskite is a new paradigm in photovoltaics, with the possibility to surpass current technology's performance constraints, achieve low cost and high efficiency and attain substantial stability. Although efficiencies of over 22 percent have recently been reported, yet not so much is known about their operational characteristics under thermal stress. Thermal stability of the Methylammonium Lead Iodide Perovskite Solar Cell was explored by investigating the influence of high temperature on the model. A promising result was achieved with Power Conversion Efficiency (PCE) of 29.31%, Fill Factor (FF) 82.63 %, short-circuit current density (J_{SC}) 23.55 mA/cm^2 and open circuit voltage (V_{OC}) 1.51 V. The Solar Cell Capacitance Simulator (SCAPS-1D) was used to simulate the modeled perovskite solar cell under various temperature ranges, and it revealed that at higher temperatures, the solar cell's carrier concentration, band gaps, electron and hole mobilities were affected, resulting in lower power conversion efficiency. In contrast to the nominal trend of recoded models having their best efficiencies at temperatures (measured in Kelvin, K) 300K before consistently decreasing, the Power Conversion Efficiency of this model appreciated above 300K, peaking at 29.3445 percent at 325K and remaining high through 355K. The findings will serve as a useful reference for fabricating and constructing thermally stable and high power conversion efficiency perovskite solar cells.*

Key Words: ***Perovskite Solar Cell, Power Conversion Efficiency, Thermal Stability, high temperature, (SCAPS-1D)***

1.INTRODUCTION

The superior qualities of solar energy in contrast to other types of energy generation has shown it could be the ultimate answer to the ever increasing human demand for energy on the planet today and in the foreseeable future [1], [2]. Only a portion of the sun's energy that irradiates the Earth's surface could be converted to provide the whole human energy supply [3]. The recent inclination towards clean and renewable energies, especially solar, hinges on the fact that it is grossly underutilized. According to an estimate by Smill in 2005, overall human mean annual power consumption is 13 Terawatts (up to 18TW in 2015), whereas the sun delivers 122 Petawatts (1 Petawatt = 10^{15} watts), far exceeding human demands. According to International Energy Agency (2018), fossil fuels such as oil, coal, and natural gas account for more than 80% of global energy consumption; with nuclear power, hydroelectric power, solar power, and other established or emerging renewable energy sources accounting for the remainder [4].

Among these alternative sources of energy, solar energy has huge progress in producing electricity through the photovoltaic process. Photovoltaic (PV) is a sub-set of solar energy conversion technology that transfers solar radiation from photons to electrons in a straightforward manner. It is a more environmentally friendly and a long-term sustainable source of energy that is based on nearly endless resources. In addition, it exploits a phenomenon that spontaneously occurs in nature [5]. The photoelectric effect, formerly known as the "Becquerel effect," is the primary principle behind the photovoltaic phenomenon. Alexandre Edmond Becquerel, a French scientist, discovered the photovoltaic phenomenon in 1839. Since then, researchers have never stopped looking into how solar cells may be transformed from a scientific curiosity to a viable energy source that can be widely distributed and effectively used in society [6].

Despite its numerous advantages, solar energy has few limitations. Sharma et al., (2015) and Bertolli, (2008) noted that though the solar energy is freely available, there is still an initial expenditure on the equipments for harvesting its energy by developing solar cells, panels and modules. Secondly, solar energy does not radiate at night. There must be plenty of sunlight available to generate electrical energy from a solar photovoltaic device. Thus, to overcome the demerits of this technology, solar energy must be stored elsewhere at night and ***highly efficient solar cells and modules*** need to be developed.

1.1 Advances in Photovoltaic Technology

As at 2014 after several years of progress, crystalline silicon technology had dominated the global PV market with 55% and 36% market shares for polycrystalline and monocrystalline silicon modules respectively. The remaining 9% of the market was split between a variety of other established and emerging PV technologies [9]. To gain market share from crystal silicon solar cells, alternative technologies will have to provide an impeccable combination of high power conversion efficiency (PCE), low manufacturing costs

and excellent stability in different environmental conditions [10]. Other technologies include established and emerging PV technologies of which Organometal Trihalide Perovskite is a promising candidate with strong promise of being among the profitable alternatives in PV business because of its high efficiency and reduced low fabrication costs.

Low solar material efficiency basically implies that producing substantial electricity would need a very big panel area. As a result, any material with a power conversion efficiency of less than 20% is regarded a poorer contender for large-scale energy generation, however it may be viable for local markets [11]. The current commercial cell efficiency record for solar cells with silicon as the basis (SSCs) is 25% [12]. This raises the question of whether all future capacity will be constructed with SSCs or other alternative solar cell materials. For some materials, such as Gallium Arsenide (GaAs), the answer appears to be negative, due to the inconvenient demand for large production facilities with expensive and high-temperature procedures, despite having high PCE of 46% for GaAs-based concentrators (figure 1) [13]; the relatively low power conversion efficiency (12 percent) of the most common Silicon-based thin film solar cells; and the inherent problems associated with the manufacturing process, which include requiring a lot of heat energy in producing the crystalline silicon structure. Furthermore, rare/scarce and poisonous elements are commonly used in materials like Cadmium Telluride (CdTe), Copper Indium Selenide (CIS), Copper Indium Gallium Selenide (CIGS), and Silicon Tetrachloride. After the quick introduction of perovskite solar cells (PSCs), which are structured solar cells made mostly of organic and plentiful materials that are environmentally beneficial, the answer becomes even more irresolute [14]; [15]; [16]. Despite its outstanding properties and even greater efficiencies, the perovskite solar cells have yet to be commercialized due to material instability. One of these issues stems from the fact that perovskite's ecological adaptability is weakened at even slightly higher temperatures (thermal instability), thus limiting its efficiency severely.

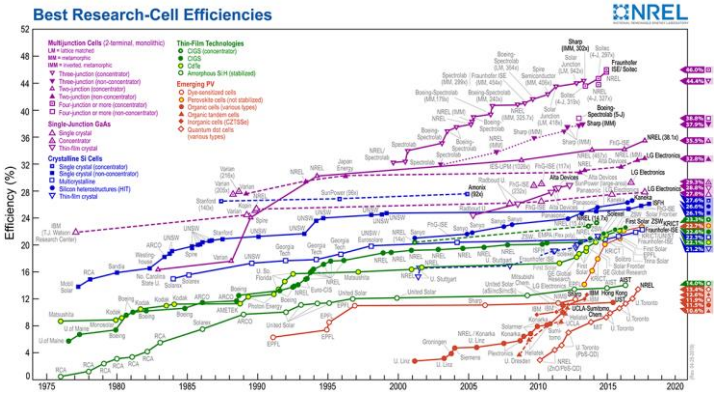

Fig -1: Research-cell efficiencies over the years certificated by NREL [13]

1.2 Features of perovskite solar cells

Perovskite is the technical name for the Calcium Titanate ($CaTiO_3$) mineral, which was discovered in 1839 by German mineralogist Gustav Rose and named after Aleksevich Von Perovski, a Russian mineralogist. Because the perovskite or perovskite-related structure may be found in a wide range of materials, it has become a generic name for crystals with this structure. Perovskites are minerals with a crystal structure similar to $CaTiO_3$ but are in a different phase transition. Perovskite crystals usually have the stoichiometry ABX_3, where A is a big organic Methylammonium (MA) or inorganic Cesium (Cs) or Rubidium (Rb) cation. B is a smaller divalent inorganic metal cation than A; like (Cu^{2+}, Sn^{2+} and Pb^{2+}), where X_3 is a halogen group monovalent anion (such as Cl^-, Br^- and I^-) that can attach to both cations A and B [17]. As illustrated in figure 2, the atoms are organized in a cubic lattice.

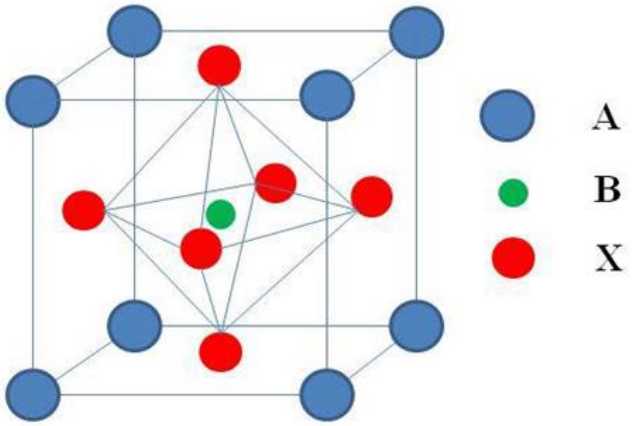

Fig -2: Cubic structure of perovskites [18].

2. LITERATURE REVIEW

Owing to their unique features, perovskite solar cells have been billed as the next big thing in photovoltaics/renewable energy space and have been extensively investigated throughout time [19]. Perovskites' efficiency has soared in recent years, from a modest 2.6 percent in 2006 [20] to over 22 percent in 2017 [21], with plenty of opportunity for improvement in the next years. Band gap engineering, compositional engineering, and contact engineering, among other creative methodologies, have enabled these advancements.

Band gap Engineering allows perovskites' band gap to be tuned throughout a wide range of the solar spectrum. Tandem perovskite cells [22], mixed halides [23] [24]; [25]; [26] [27], hybrid components like the absorber (double or triple absorbers) [28], hybrid charge-transport layers (double HTL or ETL), ETL/HTL-Free perovskite cells [29], etc. are all examples of this engineering. The addition of halides to perovskite improves its stability. Noh and colleagues demonstrated that mixing 20 percent to 29 percent Br into $CH_3NH_3PbI_3$ increased solar cell stability significantly [25]. Rolland and his colleagues investigated whether a tandem solar cell could use the same perovskite absorber material. The photovoltaic efficiency of the corresponding optimal tandem cell was 27%, which was significantly higher than the efficiencies of absorber materials alone [22].

Compositional Engineering allows for the replacement of constituent materials in whole or in part. Compositional Engineering allows for cation alloys in site-A of organic Methylammonium and Formamidinium or Cesium, cation alloys in site-B of Lead (Pb) and Tin (Sn), and combinations of Iodine halide with Bromine or Chlorine [30]. For more stable perovskite absorbers, triple cation (Cs/MA/FA) arrangement has been realized in a few situations [31]. It has been attempted to make lead-free perovskites by completely substituting lead with other group IVA elements such as Germanium (Ge) and Tin (Sn). $CsGeCl_3$ (Cesium Germanium Chloride) and MAGeCl3 (Methylammonium Germanium Chloride) are examples of germanium-based perovskites [32]. A mixed-(Tin & Lead) perovskite has also been demonstrated to be conceivable and attainable [33].

When researching the features of electron and hole collecting electrodes and their interfaces, Contact Engineering takes center stage, since they are also crucial for increasing perovskite device performance. They contribute to the control and modification of the absorber's optoelectronic and structural characteristics [34]; [35]; [36]; [37].

The impacts of different materials and their thicknesses utilized in the architectural arrangement of perovskite solar cells- electrode contacts, charge transfer layers, and absorber layer- have been explored in several studies [37]; [38]; [39]; [40]; [41]; [42]; [43]. Various efficiencies have been observed as well. This confirms that perovskite solar cells represent the future of photovoltaic technology, since they provide a better choice for generating clean energy from the sun's ample energy at a greater efficiency. Various studies have been conducted to examine the performance of various types of perovskite solar cells, particularly those containing the Methyl Ammonium cation doped with other metal-bases such as lead (Pb), tin (Sn), and the anions Bromine (Br), Chlorine (Cl) and Iodine (I) [24]; [25]; [26]; [44]; [45]; [46]; [47]; [48]. Combinations containing at least two (2) anions in various proportions, as well as various metal bases, have been examined and varying efficiencies reported with considerable interest.

Despite several achievements in the field of perovskites, there are still more problems than answers in terms of instability. Thermal instability is an albatross of perovskite solar cells, which are made up of more than one kind of material and have heterojunction properties. High temperatures target the multi-layered junctions, forcing them to operate as separate materials. As a result, significant resistance develops at each layer, obstructing electron and hole mobility. High rates of recombination at the interfaces, as well as the bulk of the materials, precede this. All semiconductor devices, including photovoltaic cells, are very temperature sensitive. The efficiency and power production of a solar cell decline as its temperature rises. This is due to increased carrier concentrations, which result in higher internal carrier recombination rates.

The impact of solar cell module temperature on photovoltaic system behavior cannot be emphasized, since it impacts the efficiency and output energy of the system. Thermal instability has resurfaced, and it is necessary to investigate the influence of temperature on the performance of perovskite solar cells in order to address this issue; and also develop ways of improving the prevalent condition.

3. MATERIALS AND METHODS

3.1 Modeling of the Perovskite Solar Cell

When a semiconducting material is illuminated by light, such material can be excited. If the material is then illuminated with photons of equal or higher energy than its energy gap, the photons can be absorbed to excite electrons from the valence band to the conduction band, allowing for current flow. The maximum current density is then given by the flux of photons with this energy. Light here, refers to an electromagnetic radiation that consists of photons and each photon carries with it a specific energy depending on its wavelength with the following relation,

$$E = \frac{hc}{\lambda} \quad (1)$$

Where;

E is the energy of the photon,
h is planks constant,
c is the speed of light and
λ is the wavelength of the photon

Figure 3 depicts the conventional circuit for solar cell electrical characterization. It describes the device's output characteristics as well as fundamental metrics like as short-circuit current, open-circuit voltage, fill factor, and power conversion efficiency (PCE).

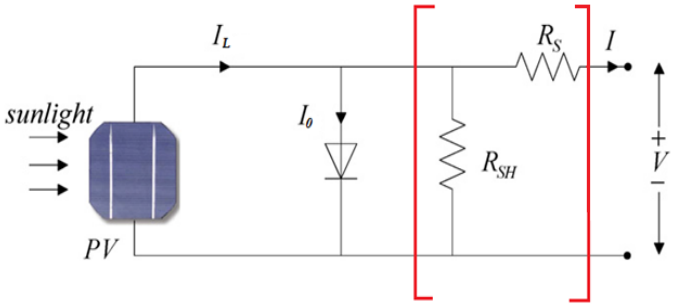

Fig -3: Schematic of an ideal solar cell and a more realistic solar cell.

In the dark and under light, the associated current-voltage (J-V) properties are shown (Figure 4). Due to the lack of light, a photovoltaic cell seems to be inactive in the dark (solar radiation). Electrical power may be collected from the fourth quadrant when light shines on the photovoltaic cell. The shaded region indicates the maximum power. The maximum output power (P_m) above the illumination power is described as the Power Conversion Efficiency (PCE).

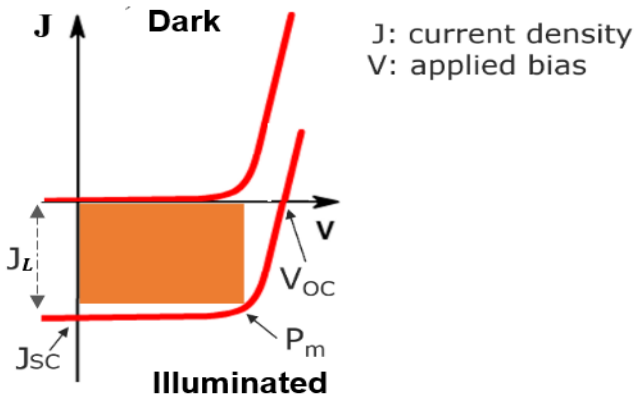

Fig -4: J-V characteristic of photovoltaic cell under illuminated and dark conditions.

During device simulation, all of the main input parameters must be accurately described in order to generate a model that acts like an actual equivalent. The system must first be modeled before the simulation can begin. Modeling is the process of creating a design or representation for the implementation of a physical system using mathematical formulae. SCAPS-1D (Solar Cell Capacitance Simulator), AMPS (Analysis of Microelectronic and Photonic Structures), COSMOL, GPVDM, SILVACO, TCAD, AFORS-HET (Automat FOR Simulation of HETerostructures), ASA (Amorphous Semiconductor Analysis), and more applications are used to simulate solar cells. Because of its unique capabilities and the substantial literature on solar device modeling and performance analysis, SCAPS-1D is employed in this study. The fundamental theory of SCAPS-1D, according to Burgelman et al., (2020), is to solve Poisson's equation and continuity equations that are difficult to answer directly using standard methods.

The theoretical model of a Perovskite Solar Cell is made up of three (3) main differential equations:

(a) Poisson's equation.
(b) Transport equation, and
(c) Continuity equation.

The performance of a perovskite solar cell in one dimension may be explained using Poisson's equation and continuity equations. Poisson's equation explains the relationship between electric potential and charge density. It's worded like this:

$$\Delta\Psi = -\frac{\rho}{\varepsilon} \quad (2)$$

Where;
Ψ is electrostatic potential
ε is dielectric constant
ρ charge density
Continuity equations are used to define the conservation of free electrons and free holes in a solar device. To comprehend non-equilibrium processes, one must also solve the electron and hole continuity equations. These are written as

$$\frac{\partial n}{\partial t} = \frac{1}{q} div\overrightarrow{J_n} + G_n - R_n \quad (3a)$$

$$\frac{\partial p}{\partial t} = -\frac{1}{q} div\overrightarrow{J_p} + G_p - R_p \quad (3b)$$

Where;
J_n is electron current density
J_p is hole current density
Gs are optical generation rates
Rs are recombination rates
n and *p* subscripts are for electron and hole respectively
t is time

Diffusion current and drift current induced by electron and hole mobility are included in the output current of a perovskite solar cell. These characterize the mobility of free electrons and holes in relation to current quasi-Fermi level location data for electrons and holes. They are as follows:

$$\overrightarrow{J_n} = J_{diffusion} + J_{drift} = q\mu_n n\vec{E} + qD_n\bar{\nu}n \quad (4a)$$

$$\overrightarrow{J_p} = J_{diffusion} + J_{drift} = -q\mu_p p\vec{E} + qD_p\bar{\nu}p \quad (4b)$$

Where;
J_n is electron current density
J_p is hole current density
E is the electric field
μ_n is electron mobility and
μ_p is hole mobility
n and p are free electrons and holes density,
E_{Fn} and E_{Fp} are electron and hole quasi-Fermi level respectively.
D_n and D_p are diffusion coefficient of electrons and holes

The Diffusion lengths of the charge carriers define the transport ability of carriers (electrons and holes) in a solar cell device. It is determined by the carrier lifetime and diffusion coefficient. which may be represented in the following way:

$$L_n^{Diff} = [D_n\tau_n]^{\frac{1}{2}} \quad (5a)$$

electron diffusion length.

$$L_p^{Diff} = [D_p\tau_p]^{\frac{1}{2}} \quad (5b)$$

hole diffusion length.

Where;
L is diffusion length,
τ is carrier lifetime
$D_n = kT_n\mu_n$ is electron diffusion coefficient,
$D_p = kT_p\mu_p$ is hole diffusion coefficient,
K is Boltzmann constant

T is spatially varying electron and hole temperature,
μ_n is electron mobility and μ_p is hole mobility
n and p are free electrons and holes density.

The Boltzmann distribution governs the density of electrons and holes at the cathode and anode, and the carrier concentration equations describe this. The charge densities of free electrons and holes in thermal equilibrium, represented by n and p, are calculated as follows:

$$n = N_C \, exp\left(\frac{E_F - E_C}{kT_n}\right) = N_C \, exp\left(\frac{V_n}{kT_n}\right) \quad (6a)$$

$$p = N_C \, exp\left(\frac{E_V - E_F}{kT_p}\right) = N_C \, exp\left(\frac{V_p}{kT_p}\right) \quad (6b)$$

Where;
E_F is Fermi level and
E_c and E_V are conduction and valence band energy levels at steady state,
N_C is the intrinsic carrier density
V is built-in potential,
K is Boltzmann constant
T is spatially varying electron and hole temperature.

When a photon of wavelength λ and intensity I[λ] illuminates an absorbent medium with thickness d, some of the energy is reflected (R), some is absorbed (A), and the rest is transmitted (T). The absorption coefficient [α(λ)] and absorbance [A_{abs} (λ)] are defined as:

$$A_{abs}(\lambda) = -\log_{10}\left[\frac{T(\lambda)}{I(\lambda) - R(\lambda)}\right] \quad (7)$$

$$\alpha(\lambda) = \frac{A_{abs}(\lambda)}{d} = \left(A + \frac{B}{h\nu}\right)\sqrt{h\nu - E_{gap}} \quad (8)$$

Where;
A and B are the absorption constants
α is optical absorption constant
λ is wavelength of photon
h is Planck's constant,
v is light speed; [*hv* is photon energy]
E_{gap} is the actual band gap of the material

When the device is exposed to light, all of the charge carriers in the device will migrate to their respective electrodes, and electrons and holes will try to recombine as they travel. In the bulk of the layer, three types of recombination processes can be introduced: defects/Shockley-Read-Hall (SRH), band-to-band/radiative, and Auger recombinations.

Shockley-Read-Hall (SRH) recombination, also known as trap-assisted recombination, happens as a result of inherent faults or imperfections in the materials. The following formula is used to calculate the rate of SRH recombination:

$$U_{SRH} = \frac{V\sigma_n\sigma_p N_T\left[np - n_i^2\right]}{\sigma_p[p + p_1] + \sigma_n[n + n_1]} \quad (9)$$

Where;
σ_n and σ_p are capture cross-sections for electrons and holes,
v is electron thermal velocity,
N_T is number of gap states per volume
n_i and p_i are intrinsic carrier concentrations of electrons and holes,

The process of photon absorption in reverse is referred to as "radiative recombination" or "Band-to-Band recombination." The conduction band's electrons return to the valence band's empty space, where they recombine with holes. The rate of radiation recombination is calculated as follows:

$$U_{radiative} = K(np - n_i^2) \quad (10)$$

Where;

$$n_i = N_C \, exp\left(-\frac{E_{gap}}{2v}\right)$$

$$K = \frac{g_{th}^R}{n_i^2}$$

Where;
K = recombination coefficient
v = electron thermal velocity,
N_C = conduction band effective density of states
n_i = intrinsic carrier concentration,
E_{gap} = the actual band gap of the material
g_{th}^R = the number of electrons in conduction band and holes in valence band generated per unit time per unit volume

The recombination of electron and hole pairs as they move from a high to a low energy state, with the energy transmitted to the third carrier, is known as Auger recombination. The following is a description of it:

$$U_{Auger} = \left(c_n^A n + c_p^A p\right)(np - n_i^2) \quad (11)$$

Where;
n_i is intrinsic carrier concentration,
c_n^A and c_p^A are constants

The density of states in the conduction and valence bands, as well as the diffusion coefficient and the thermal velocities of electrons and holes, are all affected by temperature. Both direct and indirect band gaps in bulk semiconductors are temperature dependent variables, with the functional form being fitted to the empirical Varshni law [50]. The following is the Varshni law for energy bandgap:

$$E_{gap}(T) = E_0 - {}^{\alpha T^2}/_{(T+\beta)} \quad (12)$$

Where;
A and β are adjustable Varshni parameters (constants)
T is spatially varying electron and hole temperature.
E_0 is the band gap at temperature = 0K
E_{gap} is the actual band gap of the material

V_{th} which is a function of the spatially changing electron and hole temperature in active regions, is defined as follows :

$$V_{th}(T) = \frac{V_{th}(T_0)}{T_0{}^2 * T^2}$$

Where;
T is spatially varying temperature
T_0 = default temperature = 300K

The following are the relative densities of states in the conduction and valence bands:

$$N_c = N_c(T_0)\left[\frac{T}{T_0}\right]^{1.5} \quad (10)$$

$$N_v = N_v(T_0)\left[\frac{T}{T_0}\right]^{1.5} \quad (11)$$

Where;
N_c is conduction band densities of state
N_v is valence band densities of state
T is desired temperature
T_0 = default temperature = 300K

3.2 DEVICE STRUCTURE AND SIMULATION PARAMETERS

The block design of architecture employed in the simulator's modeling of the perovskite solar cell is shown in Figure 4. In its most basic form, it represents a four-layer planar heterojunction arrangement. The device designs that follow the direction of incident light include Glass + Transparent Conducting Oxide (SnO_2:F), n-type Electron Transportation Layer (TiO_2), Absorber layer/Perovskite Material ($CH_3NH_3PbI_3$), p-type Hole Transportation Layer (Spiro-OMETAD), and Back Contact (Gold).

The model of the perovskite solar cell built by SCAPS-1D software is displayed on the Solar cell definition panel, as illustrated in Figures 5 below. Red represents a p-type material, whereas blue denotes an n-type material, according to the discretization of the structure.

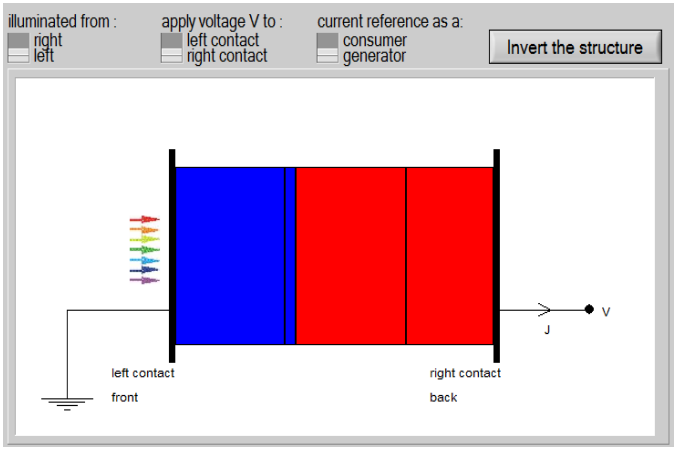

Figure 5: *The block diagram as built by SCAPS-1D software*

3.3 BASELINE PARAMETERS FOR SIMULATION

The baseline material characteristics for each layer used in this investigation are listed in Table 1 and are based on experimental data from the literature. The concentrations of the donor and acceptor are given by N_D and N_A, respectively. ε_r stands for relative permittivity; χ represents electron affinity; Eg denotes bandgap; μ_n and μ_p signify electron and hole mobilities; N_t denotes defect density; CB and VB denote effective density of states in the conduction and valence bands, respectively. Other modeling factors include the thermal velocity of electrons and holes, as well as the capture cross section of electrons and holes.

SCAPS-1D has been utilized to simulate the solar cell with charge carrier loss processes in PSCs (Bulk defect levels of $1X10^{15}$ for each layer except the absorber layer with $2.5X10^{13}$ and interface trap defect densities). Deep insights have been gained through modeling physical processes, which aids in establishing the solar cell's characteristics at high temperatures

Table -1: Baseline Parameters for Simulation

Characteristics	SnO_2: F	TiO_2	$CH_3NH_3PbI_3$	Spiro-OMeTAD
Thickness (μm)	0.5	0.05	0.5	0.4
Band gap (eV) Eg	3.5	3.2	1.55	2.91
Electron affinity (eV) χ	4.0	4.0	3.9	2.2
Dielectric permittivity ϵ_r	9.0	100	30	3
CB effective density of states ($1/cm^3$)	$2.20X10^{17}$	$2.0X10^{18}$	$2.2X10^{15}$	$2.5X10^{18}$
VB effective density of states ($1/cm^3$)	$2.20X10^{16}$	$1.0X10^{19}$	$2.2X10^{17}$	$1.8X10^{19}$
Electron thermal velocity (cm/s)	$1X10^7$	$1.0X10^7$	$1.0X10^7$	$1.0X10^7$
Hole thermal velocity (cm/s)	$1X10^7$	$1.0X10^7$	$1.0X10^7$	$1.0X10^7$

Electron mobility (cm^2/Vs)	20	$2.0X10^4$	2	$2.0X10^{-4}$
Hole mobility (cm^2/Vs)	10	$1.0X10^3$	2	$2.0X10^{-4}$
Shallow uniform donor density N_D ($1/cm^3$)	$1X10^{19}$	$5.0X10^{19}$	0	0
Shallow uniform acceptor density N_A ($1/cm^3$)	0	0	$1.0X10^{13}$	$3.0X10^{18}$
Total Defect Density N_T (cm^{-3})	$1X10^{15}$	$1X10^{15}$	$2.5X10^{13}$	$1X10^{15}$

4. RESULTS

Temperature dependence was applied to all other parameters to represent the impact of temperature on the modeled perovskite solar cell (which is the desired temperature levels). To do this, the temperature (K) was declared as a batch parameter in the Batch Set-up. To better understand and quantify the impact of temperature on the performance of the perovskite solar cell, simulations were ran at different temperatures (measured in Kelvin, K), T = 275K - 450K, with a step increase of 25K.

4.1 RESULT OF REFERENCE MODEL

In both dark and light situations, device characteristics were investigated. The dark current is depicted by the RED line in figure 6, whereas the current under light is depicted by the BLUE trace. In the absence of illumination (dark), the solar cell behaved like a gigantic flat diode, producing very little current and little or no generated charges. When the solar cell is lighted, charges produced by light photons cause current to flow, and the solar cell begins to operate. The J-V curve of the simulated model was shown in blue, with all of the pre-set parameters as follows: maximum power conversion efficiency is 29.31 percent, FF=82.63 percent, Jsc= 23.55mA/cm^2, Voc=1.51V.

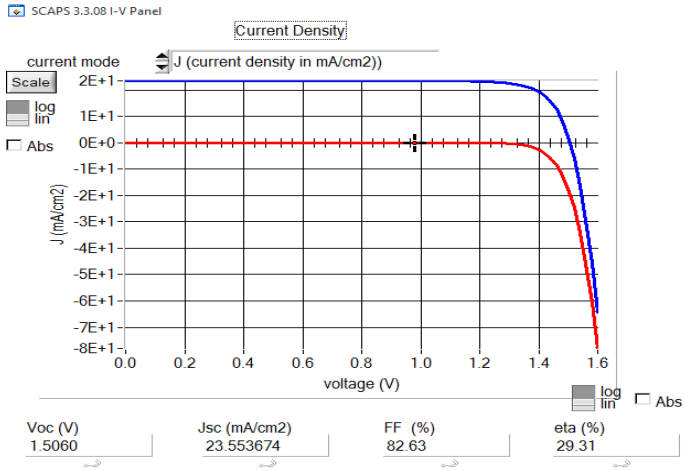

Figure 6: The Dark and Illuminated *J-V* Characteristics of the PSC model

4.2 Effect of Temperature on Performance of the Perovskite Solar Cell

In simulation studies and fabrications, 300K is commonly utilized as the working temperature since it is considered room temperature, albeit this is not always the case in the open field. Solar cells frequently operate at temperatures above 300K. As a result, to better understand the impacts of operating temperature on cell performance, the operating temperature domain in this study has been established from 275K to 450K with a 25K step increase.

Table -1: Dependence of solar cell performance on the Operating Temperature

T (K)	Jsc (mA/cm^2)	Voc (V)	FF (%)	PCE (%)
275	23.553393	1.4973	82.8975	29.2360
300	23.553674	1.5060	82.6322	29.3119
325	23.553964	1.5102	82.5961	29.3445
350	23.554255	1.5105	82.3365	29.2942
375	23.554491	1.5078	82.1643	29.1803
400	23.554631	1.5027	81.8109	28.9570
425	23.554926	1.4957	81.4477	28.6954
450	23.555224	1.4874	80.9585	28.3637

The electrical properties of the PSC model are shown against temperature in Charts 1 to 3. While the J_{SC} was continually increasing, the V_{OC}, FF, and PCE were decreasing. This demonstrates that as the operational temperature grew, the solar model's performance worsened. This is because greater temperatures affect the solar cell's carrier concentration, band gaps, electron, and hole mobilities, resulting in lower conversion efficiency. V_{OC} dropped as temperature climbed because short circuit current is temperature dependant. The rise in short circuit current is mostly to blame for the decrease in V_{OC}. This is due to the fact that higher operating temperatures provide more energy to electrons. Electrons get more energy and have a higher level of entropy at higher temperatures. They become very unstable, and are more likely to recombine with the holes before reaching the electrode contacts. These findings are consistent with those of Devi et al., (2018), discovered that electron and hole mobility, carrier concentration, and bandgap are all affected by high temperatures. As a result, as the findings of this simulation show, ambient temperature, which has a direct influence on device temperature, has a considerable impact on cell performance.

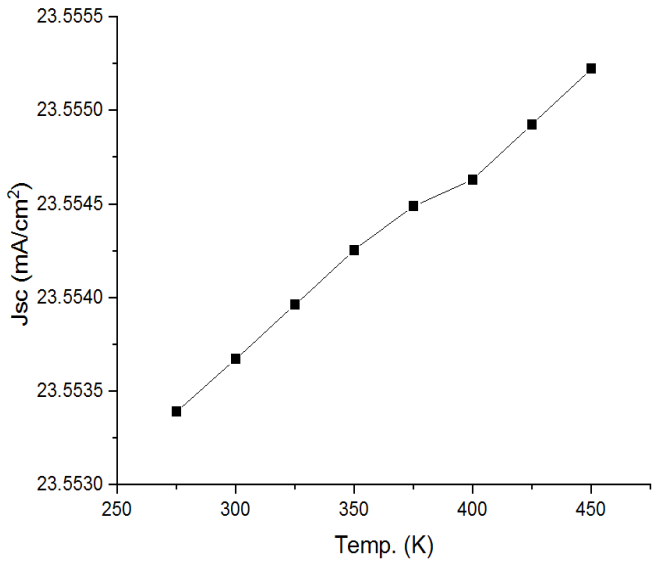

Chart -1: Variation in J_{SC} of PSC model with operating temperature.

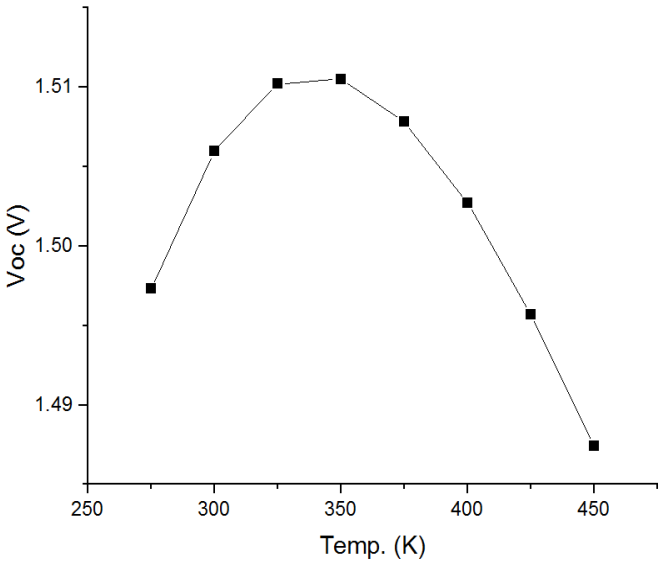

Chart -2: Variation in V_{OC} of PSC model with operating temperature.

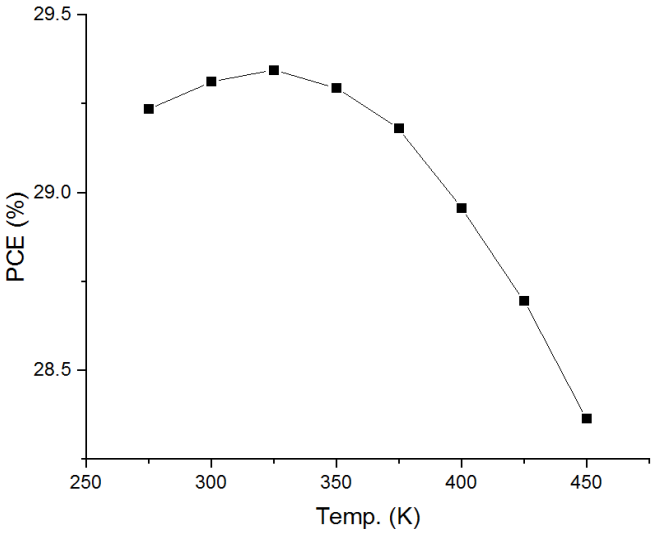

Chart -3: Variation in Efficiency of PSC model with operating temperature.

As can be seen in the charts above, the implemented model showed better performance in contrast to the conventional trend where cell efficiency capitulates and takes a negative trend or, in the best case scenario, remains constant for a very short time before declining. V_{OC} and PCE in this model appreciated to a point (325K and 355K) above 300K before dropping. This shows that this model has the ability to endure thermal disturbances in these temperature ranges above the typical operating temperature. It is a milestone in photovoltaic research that stand-alone perovskite solar modules running successfully at temperatures beyond 300K and up to 355K are not only conceivable, but also possible and achievable

5. CONCLUSION

The influence of high temperature on the performance of a Methylammonium lead iodide perovskite solar cell was investigated in this work using numerical modeling of the solar cell. The device was modeled, simulated, and analyzed using the Solar Cell Capacitance Simulator (SCAPS). The device model produced the following results: a short-circuit current density (Jsc) of 23.55 mA/cm², an open circuit voltage (Voc) of 1.51 V, a Power Conversion Efficiency of 29.31 percent, and a Fill Factor (FF) of 82.63 percent. Temperature investigation found that the model's V_{OC} and PCE increased between 325K and 355K, above the 300K standard threshold before reducing. This clearly demonstrates that the model can resist thermal perturbations within these high temperature ranges. The results from this work will give a valuable guideline to engineers and researchers in finding best possible ways to design and produce thermally stable, high-efficiency perovskite solar cells.

DATA AVAILABILITY

The authors declare that the main data supporting the findings of this study are available within the article. Extra data are available from the corresponding author upon reasonable request.

ACKNOWLEDGEMENT

This work is (partially) supported through the Africa Centers of Excellence for Development Impact (ACE Impact) project.

The authors gratefully acknowledge Prof. Marc Burgelman and his team at the Department of Electronics and Information Systems (ELIS), University of Gent, Belgium for providing the SCAPS-1D simulation program.

REFERENCES

[1] A. Sahu, N. Yadav, and K. Sudhakar, "Floating photovoltaic power plant : A review," Renew. Sustain. Energy Rev., vol. 66, pp. 815–824, 2016, doi: 10.1016/j.rser.2016.08.051.

[2] A. Modi, F. Bühler, J. G. Andreasen, and F. Haglind, "A review of solar energy based heat and power generation systems," Renew. Sustain. Energy Rev., vol. 67, pp. 1047–1064, 2017, doi: 10.1016/j.rser.2016.09.075.

[3] F. Brivio, "Atomistic modelling of perovskite solar cells Atomistic modelling of perovskite solar cells," University of Bath, 2016.

[4] International Energy Agency, "World Energy Outlook 2018 The Gold Standard of Energy Analysis," 2018. .

[5] M. Jarraud and A. Steiner, "Summary for policymakers," in Managing the Risks of Extreme Events and Disasters to Advance Climate Change Adaptation: Special Report of the Intergovernmental Panel on Climate Change, vol. 9781107025, 2012, pp. 3–22.

[6] Y. Huang, "Drift diffusion Modelling of perovskite based solar cells , III-V optoelectronic devices and Kelvin probe force microscopy," Université Bretagne Loire, INSA de Rennes, 2018.

[7] S. Sharma, K. K. Jain, and A. Sharma, "Solar Cells : In Research and Applications — A Review," Mater. Sci. Appl., vol. 6, pp. 1145–1155, 2015, doi: 10.4236/msa.2015.612113.

[8] M. Bertolli, "Solar Cell Materials," 2008.

[9] M. A. Green, K. Emery, Y. Hishikawa, W. Warta, and E. D. Dunlop, "Solar cell efficiency tables (version 47)," Prog. Photovoltaics Res. Appl., vol. 24, no. 1, pp. 3–11, 2016, doi: 10.1002/pip.

[10] Z. Song, S. C. Watthage, A. B. Phillips, and M. J. Heben, "Pathways toward high-performance perovskite solar cells : review of recent advances in organo-metal halide perovskites for photovoltaic applications," J. Photonics Energy, vol. 6, no. 2, 2016, doi: 10.1117/1.JPE.6.022001.

[11] J. Bisquert, E. Juarez-Perez, and P. V. Kamat, "Hybrid Perovskite Solar Cells . The Genesis and Early Developments , 2009-," Fund. SCITO, pp. 2009–2014, 2017.

[12] P. J. Cousins et al., "Generation 3: improved performance at lower cost." pp. 275–278, 2010, doi: doi:10.1109/PVSC.2010.5615850.

[13] N. E. Chart, "Best research cell efficiencies," NREL Efficiency Chart, 2012. [Online]. Available: http://www.nrel.gov/ncpv/images/efficiency_chart.jpg.

[14] M. Gratzel, "The Rise of Highly Efficient and Stable Perovskite Solar Cells," Acc. Chem. Res., vol. 50, no. 3, pp. 487–491, 2017, doi: 10.1021/acs.accounts.6b00492.

[15] W. Zhang, G. E. Eperon, and H. J. Snaith, "Metal halide perovskites for energy applications," Nat. Energy, vol. 1, no. 16048, pp. 1–8, 2016, doi: 10.1038/NENERGY.2016.48.

[16] W. S. Yang et al., "High-performance photovoltaic perovskite layers fabricated through intramolecular exchange," Sol. CELLS, vol. 348, no. 6240, pp. 1234–1237, 2015, doi: https://doi.org/10.1126/science.aaa9272.

[17] S. Luo and W. A. Daoud, "Recent progress in organic-inorganic halide perovskite solar cells: Mechanisms and material design," J. Mater. Chem. A, no. November, pp. 1–19, 2014, doi: 10.1039/C4TA04953E.

[18] J. Stenberg, "Perovskite solar cells," Umea University, 2017.

[19] H. J. Snaith, "Present Status and Future Prospects of Perovskite Photovoltaics," Nat. Mater., vol. 17, pp. 372–376, 2018.

[20] A. Kojima, K. Teshima, Y. Shirai, and T. Miyasaka, "Novel Photoelectrochemical Cell with Mesoscopic Electrodes Sensitized by Lead-halide Compounds.," in 210th ECS Meeting, 2006, no. 2, p. 397, doi: 10.1149/ma2007-02/8/352.

[21] O. K. Simya, A. Mahaboobbatcha, and K. Balachander, "Compositional grading of CZTSSe alloy using

exponential and uniform grading laws in SCAPS-ID Simulation," Superlattices Microstruct., vol. 92, pp. 285–293, 2016, doi: 10.1016/j.spmi.2016.02.019.

[22] A. Rolland et al., "Computational design of high performance hybrid perovskite on silicon tandem solar cells," 2016.

[23] M. Abdi-jalebi et al., "Maximizing and stabilizing luminescence from halide perovskites with potassium passivation," Nature, vol. 555, no. 7697, pp. 497–501, 2018, doi: 10.1038/nature25989.

[24] S. D. Stranks et al., "Electron-hole diffusion lengths exceeding 1 micrometer in an organometal trihalide perovskite absorber," Science (80-.)., vol. 342, no. 6156, pp. 341–344, 2013, doi: 10.1126/science.1243982.

[25] J. H. Noh, S. H. Im, J. H. Heo, T. N. Mandal, and S. Il Seok, "Chemical management for colourful, efficient and stable inorganic - organic hybrid nanostructured solar cells," Nano Lett., vol. 13, p. 1764–1769, 2013.

[26] E. Edri et al., "Why lead methylammonium tri-iodide perovskite-based solar cells require a mesoporous electron transporting scaffold (but not necessarily a hole conductor)," Nano Lett., vol. 14, no. 2, pp. 1000–1004, 2014, doi: 10.1021/nl404454h.

[27] B. Suarez, V. Gonzalez-Pedro, T. S. Ripolles, R. S. Sanchez, L. Otero, and I. Mora-Sero, "Recombination study of combined halides (Cl, Br, I) perovskite solar cells," J. Phys. Chem. Lett., vol. 5, no. 10, pp. 1628–1635, 2014, doi: 10.1021/jz5006797.

[28] I. T. Bello and M. K. Awodele, "Modeling and simulation of CZTS-perovskite sandwiched tandem solar cell," Turkish J. Phys., vol. 48, pp. 321–328, 2018, doi: 10.3906/fiz-1801-30.

[29] A. Dymshits, A. Rotem, and L. Etgar, "High voltage in hole conductor free organo metal halide perovskite solar cells," J. Mater. Chem. A, vol. 2, no. 48, pp. 20776–20781, 2014, doi: 10.1039/c4ta05613b.

[30] M. A. Green, A. Ho-Baillie, and H. J. Snaith, "The emergence of perovskite solar cells," Nat. Photonics, vol. 8, no. 7, pp. 506–514, 2014, doi: 10.1038/nphoton.2014.134.

[31] M. Saliba et al., "Cesium-containing Triple Cation Perovskite Solar Cells: Improved Stability, Reproducibility and High Efficiency," Energy Environ. Sci., vol. 9, no. 6, pp. 1989–1997, 2016, doi: 10.1039/C5EE03874J.

[32] T. Baikie et al., "Synthesis and Crystal Chemistry of the Hyrid Perovskite (CH3NH3)PBI3 for Solid-State Sensitized Solar Cell Applications," J. Mater. Chem. A, vol. 1, pp. 5628–5641, 2013, doi: 10.1039/C3TA10518K.

[33] Y. Ogomi et al., "CH3NH3SnxPb(1-x)I3 Perovskite Solar Cells Covering up to 1060nm," J. Phys. Chem. Lett., vol. 5, no. 6, pp. 1004–1011, 2014, doi: 10.1021/jz5002117.

[34] Y. Han et al., "Degradation observations of encapsulated planar CH3NH3PbI3 perovskite solar cells at high temperatures and humidity," J. Mater. Chem. A, vol. 3, no. 15, pp. 8139–8147, 2015, doi: 10.1039/c5ta00358j.

[35] Y. Kato, L. K. Ono, M. V. Lee, S. Wang, S. R. Raga, and Y. Qi, "Silver Iodide Formation in Methyl Ammonium Lead Iodide Perovskite Solar Cells with Silver Top Electrodes," Adv. Mater. Interfaces, vol. 2, no. 13, pp. 2–7, 2015, doi: 10.1002/admi.201500195.

[36] L. Fagiolari and F. Bella, "Carbon-based materials for stable, cheaper and large-scale processable perovskite solar cells," Energy Environ. Sci., vol. 12, pp. 3437–3472, 2019, doi: 10.1039/c9ee02115a.

[37] A. Husainat, W. Ali, P. Cofie, J. Attia, J. Fuller, and A. Darwish, "Simulation and Analysis Method of Different Back Metals Contact of CH3NH3PbI3 Perovskite Solar Cell Along with Electron Transport Layer TiO2 Using MBMT-MAPLE/PLD," Am. J. Opt. Photonics, vol. 8, no. 1, pp. 6–26, 2020, doi: 10.11648/j.ajop.20200801.12.

[38] S. Andalibi, A. Rostami, G. Darvish, and M. kazem Moravvej-Farshi, "A Strategy to Achieve High-Efficiency Organolead Trihalide Perovskite Solar Cells," J. Electron. Mater., vol. 45, no. 11, pp. 5746–5756, 2016, doi: 10.1007/s11664-016-4772-2.

[39] A. Husainat, W. Ali, P. Cofie, J. Attia, and J. Fuller, "Simulation and Analysis of Methylammonium Lead Iodide (CH3NH3PbI3) Perovskite Solar Cell with Au Contact Using SCAPS 1D Simulator," Am. J. Opt. Photonics, vol. 7, no. 2, pp. 33–40, 2019, doi: 10.11648/j.ajop.20190702.12.

[40] F. Liu et al., "Numerical simulation: Toward the design of high-efficiency planar perovskite solar cells," Appl. Phys. Lett., vol. 104, no. 25, pp. 1–5, 2014, doi: 10.1063/1.4885367.

[41] M. Kaifi and S. K. Gupta, "Simulation of Perovskite based Solar Cell and Photodetector using SCAPS Software," Int. J. Eng. Res. Technol., vol. 12, no. 10, pp. 1778–1786, 2019.

[42] K. R. Adhikari, S. Gurung, B. K. Bhattarai, and B. M. Soucase, "Comparative study on MAPbI3 based solar cells using different electron transporting materials," Phys. Status Solidi, vol. 13, no. 1, pp. 13–17, 2016,

doi: 10.1002/pssc.201510078.

[43] F. Hossain, M. Faisal, and H. Okada, "Device Modeling and Performance Analysis of Perovskite Solar Cells Based on Similarity with Inorganic Thin Film Solar Cells Structure," in 2nd International Conference on Electrical, Computer & Telecommunication Engineering (ICECTE) 8-10 December 2016, Rajshahi-6204, Bangladesh, 2016, pp. 8–10.

[44] E. Edri, S. Kirmayer, D. Cahen, and G. Hodes, "High Open-Circuit Voltage Solar Cells Based on Orgaic-Inorganic Lead Bromide Perovskite," J. Phys. Chem. Lett., vol. 4, no. 6, pp. 897–902, 2013, doi: 10.1021/jz400348q.

[45] M. M. Lee, J. Teuscher, T. Miyasaka, T. N. Murakami, and H. J. Snaith, "Efficient Hybrid Solar Cells Based on Meso-Superstructured Organometal Halide Perovskites," Science (80-.)., vol. 338, no. 6107, pp. 643–647, 2012, doi: 10.1126/science.1228604.

[46] U. Mandadapu, S. V. Vedanayakam, K. Thyagarajan, M. R. Reddy, and B. J. Babu, "Design and simulation of high efficiency tin halide perovskite solar cell," Int. J. Renew. Energy Res., vol. 7, no. 4, pp. 1604–1612, 2017.

[47] S. Colella et al., "MAPbI3-xClx mixed halide perovskite for hybrid solar cells: The role of chloride as dopant on the transport and structural properties," Chem. Mater., vol. 25, no. 22, pp. 4613–4618, 2013, doi: 10.1021/cm402919x.

[48] E. Edri, S. Kirmayer, M. Kulbak, G. Hodes, and D. Cahen, "Chloride inclusion and hole transport material doping to improve methyl ammonium lead bromide perovskite-based high open-circuit voltage solar cells," J. Phys. Chem. Lett., vol. 5, no. 3, pp. 429–433, 2014, doi: 10.1021/jz402706q.

[49] M. Burgelman, K. Decock, A. Niemegeers, J. Verschraegen, and S. Degrave, "SCAPS manual-SCAPS version 3.3.08," no. University of Gent. pp. 1–135, 2020.

[50] Y. . Varshni, "Temperature dependence of the energy gap in semiconductors," Physica, vol. 34, no. 1, pp. 149–154, 1967, doi: https://doi.org/10.1016/0031-8914(67)90062-6.

[51] N. Devi, K. A. Parrey, A. Aziz, and S. Datta, "Numerical simulations of perovskite thin-film solar cells using a CdS hole blocking layer," J. Vac. Sci. Technol. B, vol. 36, no. 4, pp. 1–9, 2018, doi: doi:10.1116/1.5026163.

BIOGRAPHY

MBACHU, CHISOM PATRICK is a master's student in Power System Engineering, Department of Electrical/Electronic Engineering, Federal University of Technology, Owerri. He is also a research student at African Center of Excellence in Future Energies and Electrochemical Systems (ACE-FUELS), Federal University of Technology, Owerri, Nigeria. His research areas include: HVDC transmission technology, Clean and Future Energies, Climate change.